

Gene Transfer in Rodent Nervous Tissue Following Hindlimb Intramuscular Delivery of Recombinant Adeno-Associated Virus Serotypes AAV2/6, AAV2/8, and AAV2/9

Neuroscience Insights
Volume 14: 1–12
© The Author(s) 2019
Article reuse guidelines:
sagepub.com/journals-permissions
DOI: 10.1177/1179069519889022



Asad Jan¹, Mette Richner², Christian B Vægter², Jens R Nyengaard³ and Poul H Jensen²

¹Aarhus Institute of Advanced Studies and Department of Biomedicine, Aarhus University, Aarhus, Denmark. ²Danish Research Institute of Translational Neuroscience (DANDRITE), Department of Biomedicine, Aarhus University, Aarhus, Denmark. ³Core Center for Molecular Morphology, Section for Stereology and Microscopy, Department of Clinical Medicine, and Centre for Stochastic Geometry and Advanced Bioimaging, Aarhus University, Aarhus, Denmark.

ABSTRACT: Recombinant adeno-associated virus (rAAV) vectors have emerged as the safe vehicles of choice for long-term gene transfer in mammalian nervous system. Recombinant adeno-associated virus-mediated localized gene transfer in adult nervous system following direct inoculation, that is, intracerebral or intrathecal, is well documented. However, recombinant adeno-associated virus delivery in defined neuronal populations in adult animals using less-invasive methods as well as avoiding ectopic gene expression following systemic inoculation remain challenging. Harnessing the capability of some recombinant adeno-associated virus serotypes for retrograde transduction may potentially address such limitations (Note: The term *retrograde transduction* in this manuscript refers to the uptake of injected recombinant adeno-associated virus particles at nerve terminals, retrograde transport, and subsequent transduction of nerve cell soma). In some studies, recombinant adeno-associated virus serotypes 2/6, 2/8, and 2/9 have been shown to exhibit transduction of connected neuroanatomical tracts in adult animals following lower limb intramuscular recombinant adeno-associated virus delivery in a pattern suggestive of retrograde transduction. However, an extensive side-by-side comparison of these serotypes following intramuscular delivery regarding tissue viral load, and the effect of promoter on transgene expression, has not been performed. Hence, we delivered recombinant adeno-associated virus serotypes 2/6, 2/8, or 2/9 encoding enhanced green fluorescent protein (eGFP), under the control of either cytomegalovirus (CMV) or human synapsin (hSyn) promoter, via a single unilateral hindlimb intramuscular injection in the biceps femoris of adult C57BL/6J mice. Four weeks post injection, we quantified viral load and transgene (enhanced green fluorescent protein) expression in muscle and related nervous tissues. Our data show that the select recombinant adeno-associated virus serotypes transduce sciatic nerve and groups of neurons in the dorsal root ganglia on the injected side, indicating that the intramuscular recombinant adeno-associated virus delivery is useful for achieving gene transfer in local neuroanatomical tracts. We also observed sparse recombinant adeno-associated virus viral delivery or eGFP transduction in lumbar spinal cord and a noticeable lack thereof in brain. Therefore, further improvements in recombinant adeno-associated virus design are warranted to achieve efficient widespread retrograde transduction following intramuscular and possibly other peripheral routes of delivery.

KEYWORDS: Adeno-associated virus, recombinant adeno-associated virus delivery, gene delivery, nervous system

RECEIVED: August 5, 2019. **ACCEPTED:** October 15, 2019.

TYPE: Original Research

FUNDING: The author(s) disclosed receipt of the following financial support for the research, authorship, and/or publication of this article: This work was supported by funding to AJ in the form of AIAS-COFUND fellowship from European Union's Horizon 2020 Research and Innovation Programme under the Marie Skłodowska-Curie agreement (grant no. 754513) and the Lundbeckfonden, Denmark (grant no. R250-2017-1131) and supported by funding to PHJ by Lundbeckfonden Grant (grant nos DANDRITE-R248-2016-2518 and R171-2014-591). MR was funded by AUFF starting grant (grant no. AUFF-E-2015-FLS-8-4)

and JNR (Centre for Stochastic Geometry and Advanced Bioimaging) is supported by Villum Foundation.

DECLARATION OF CONFLICTING INTERESTS: The author(s) declared no potential conflicts of interest with respect to the research, authorship, and/or publication of this article.

CORRESPONDING AUTHOR: Asad Jan, Aarhus Institute of Advanced Studies and Department of Biomedicine, Aarhus University, Høegh-Guldbergs Gade 6B, DK-8000 Aarhus, Denmark. Email: ajan@aias.au.dk

Introduction

Adeno-associated viruses (AAVs) belong to the DNA *parvovirinae* family in the *Dependovirus* genus.¹ Some estimates suggest that as much as 80% of the human population is AAV seropositive^{2,3}; however, the viruses are not known to cause morbidity, making them attractive agents for applications in human gene therapy.^{1,4} The biology of AAV, putative cellular receptors for uptake, and mechanism of transduction have been studied extensively, especially for AAV2, and reviewed in details elsewhere.^{1,4} Recombinant AAV (rAAV) vectors remain the most commonly used viral vectors in neuroscience research to achieve long-term and stable gene expression.^{1,4-6} Advances in recombinant DNA technology have provided a way to

develop novel rAAV pseudotypes in which the genome and capsid components of different AAV viruses are co-packaged during virus production. For example, rAAV2/9 indicates that recombinant genome containing the AAV2-inverted terminal repeats is packaged in capsid derived from AAV9.

Recombinant AAV has been delivered into peripheral and central nervous system *in vivo* by multiple routes with variable transduction efficiencies. In adult nervous tissue, a common challenge is the efficient delivery of rAAV in select neuroanatomical areas, which is most commonly achieved by direct parenchymal (ie, intracerebral or intrathecal) injection. This mode of rAAV delivery is advantageous as it results in the highest gene expression at the site of injection, as well as



Creative Commons Non Commercial CC BY-NC: This article is distributed under the terms of the Creative Commons Attribution-NonCommercial 4.0 License (<http://www.creativecommons.org/licenses/by-nc/4.0/>) which permits non-commercial use, reproduction and distribution of the work without further permission provided the original work is attributed as specified on the SAGE and Open Access pages (<https://us.sagepub.com/en-us/nam/open-access-at-sage>).

circumvents unintended ectopic gene expression in systemic organs such as liver and heart.^{1,7,8} However, this invasive approach is associated with tissue trauma and concurrent inflammation, which could be confounding factors (eg, especially in models of chronic neurological diseases), but may also affect transgene expression.^{1,4,9} Therefore, there is burgeoning interest in evaluating minimally invasive approaches for rAAV-mediated gene delivery to nervous system by systemic inoculation (eg, rAAV9,¹⁰ or recently AAV-PHB.eB and AAV-PHP.S¹¹).

Some rAAV capsid modifications have been shown to enhance their neuronal tropism and promote retrograde transduction (The term *retrograde transduction* in this manuscript refers to the uptake of injected rAAV particles at nerve terminals, retrograde transport, and subsequent transduction of nerve cell soma.) following peripheral routes of delivery (eg, subcutaneous, s.c.; intramuscular, i.m.; intra-organ, i.o.).¹ This could present an area in rAAV development that may tremendously advance their translational utility in neuroscience, especially if rAAV could be delivered locally at a peripheral site (eg, s.c.; i.m.) to target defined neuronal populations in peripheral and/or central nervous system.¹ Furthermore, a subset of promoters has been identified, which permits generalized transgene expression in transduced tissue (eg, cytomegalovirus [CMV] promoter) or cell-type-specific expression in neurons (eg, human synapsin promoter [hSyn]) or glia (eg, glial fibrillary acidic protein [GFAP] promoter).¹² The advantages of rAAV delivery using minimally invasive peripheral routes include not only achieving gene transfer in a targeted manner but also the avoidance of tissue trauma that may influence the gene expression and study outcomes.

Among the commonly used rAAV serotypes, rAAV2/6, 2/8, and 2/9 have been shown to transduce neurons in dorsal root ganglia (DRG) and spinal cord following peripheral routes of delivery, purportedly via retrograde transduction.¹³⁻¹⁶ These rAAV serotypes have been employed by multiple research groups for transgene overexpression or delivery of gene silencing constructs in vivo by direct intraparenchymal or peripheral routes.^{1,6,12} However, an extensive side-by-side comparison of these 3 serotypes evaluating viral delivery into adult nervous tissue following a peripheral route of inoculation and the effect of promoter on transgene expression under identical experimental conditions has not been performed. In this proof-of-concept study, we performed a comparative evaluation of the 3 rAAV serotypes (ie, rAAV2/6, 2/8, and 2/9) encoding enhanced green fluorescent protein (eGFP – a useful marker widely used in similar studies for quantitative purposes and visualization^{7,13}), which were delivered using a single unilateral hindlimb i.m. injection in adult wild-type C57BL/6J mice (see section ‘Materials and Methods’). Enhanced green fluorescent protein transgene expression was driven under the control of either the CMV promoter (for achieving general transduction) or hSyn promoter (for achieving predominantly

neuron-specific transduction), thus comparing the effect of these 2 widely used promoters. To increase the possibility of targeting multiple neuronal populations, we chose to deliver rAAV into mice by i.m. route as muscle tissue is highly innervated by components of both motor and sensory systems. We anticipate that our findings will serve as useful guide to researchers who aim to employ rAAV for localized gene transfer or modulating gene expression in select neuroanatomical tracts using peripheral routes of inoculation.

Materials and Methods

Recombinant AAV production

High-purity rAAV particles of the serotypes 2/6, 2/8, and 2/9 containing CMV:eGFP or hSyn:eGFP expression cassette flanked by AAV inverted repeats were obtained from the Iowa Vector Core, Iowa University, USA.

Animal studies

All procedures were performed in accordance with Danish National rules and the European Communities Council Directive for the care and handling of laboratory animals. Wild-type (C57BL/6J) mice, 3 to 4 months of age, were housed at the Aarhus University Bartholin animal facility under conditions of 12 h light/dark cycles and received ad libitum standard laboratory chow diet. Both male and female mice were used for analyses. Mice were anesthetized with isoflurane (1%-5%) inhalation and injected intramuscularly (i.m.) with rAAV particles (2.5×10^{10} viral particles, diluted in phosphate-buffered saline [PBS]) into the right hindlimb biceps femoris muscle unilaterally using a 10- μ L Hamilton syringe (Model #801 RN) with a 25-gauge needle ($n=6$ /group). To ensure adequate inoculation, rAAV particles were injected at 3 sites in the muscle (upper part, centre of the muscle belly, and lower part) with injection volume not exceeding 3 μ L at each site. A gentle massage on the muscle was performed to facilitate the diffusion of viral particles,¹⁷ and the mice were allowed to recover under close observation before returning to their original cage. Four weeks after the rAAV injection, the mice were terminally anaesthetized i.p. with sodium pentobarbital (100 mg/kg) followed by transcardiac perfusion with ice cold PBS containing 10 000 units/L heparin (Sigma, #H3393). Then, tissues including hindlimb biceps femoris muscle (right and left sides), sciatic nerve (right and left sides, segment between sciatic notch and trifurcation in popliteal fossa), L4-L5 DRG (right and left sides), spinal cord, brain, and liver were dissected. For collecting spinal cord and subsequent dissection of DRG, an improved method based on the hydraulic extrusion of spinal cord was employed, which minimizes tissue handling and maintains the DRG integrity.¹⁸ For the determination of viral genome in the tissue and gene expression studies (see in the following), the tissues were transferred into cryogenic vials and fresh frozen in liquid nitrogen

(n=3/group). In parallel, harvested tissues were fixed in 4% paraformaldehyde (in PBS) overnight at 4°C and embedded in paraffin blocks for immunohistochemical analysis as outlined in the following (n=3/group).

Quantitative polymerase chain reaction

For the determination of viral genome in tissue, genomic DNA was extracted from the fresh frozen tissue using a commercial kit (#K0721; Thermo Fisher) following the manufacturer's protocol. Genomic DNA (10ng) was amplified with SYBR green (#4385616; Thermo Fisher) using primers targeting SV40 polyA in CMV:eGFP (forward, 5'-TGGACAAACCA CAACTAGAATGCAG-3'; reverse, 5'-CTCCCACACCT CCCCCTGAA-3') or bovine growth hormone polyA in hSyn:eGFP (forward, 5'-CCGTGCCTTCCTTGACC CTG-3'; reverse, 5'-TCCCAATCCTCCCCCTTGCT-3'), and using mouse β -tubulin (*Tubb2b*) as internal control (forward, 5'-GCCAGAGTGGTGCAGGAAATA-3'; reverse, 5'-TCACCACGTCCAGGACAGAGT-3'). All the samples were run in duplicates per experiment and average values were used for analyses. Vector genome copies were expressed for 2N genomes according to the β -tubulin copy number measured in the same sample (2 β -tubulin gene copies/cell genome¹⁹). For the determination of eGFP mRNA expression, total RNA was extracted from the fresh frozen tissue using QIAzol lysis reagent (#74134; Qiagen) and purified using a commercial kit (#74134; Qiagen). Complementary DNA (cDNA) was synthesized using high-capacity reverse transcriptase kit (#4368814; Applied Biosystems). Quantitative polymerase chain reaction (qPCR) was performed using SYBR green (#4385616; Thermo Fisher) under standard conditions with primers targeting eGFP (forward, 5'-TGACCCTGAA GTTCATCTGCACCA-3'; reverse, 5'-TCTTGTAGTTG CCGTCGTCCTTGA-3') and mouse *gapdh* (forward, 5'-CCCTTAAGAGGGATGCTGCC-3'; reverse, 5'-TAC GGCCAAATCCGTTTACA-3'). The samples were run in duplicates per experiment and average values were used for analyses. The data were analysed by relative $\Delta\Delta CT$ relative quantification method²⁰ using *Gapdh* CT values as internal reference in each sample: eGFP RNA expression = $2^{-\Delta\Delta CT}$, where $\Delta\Delta CT = \{[CT \text{ value } (egfp) \text{ Test sample} - CT \text{ value } (gapdh) \text{ Test sample}] - [CT \text{ value } (egfp) \text{ Control sample} - CT \text{ value } (gapdh) \text{ Control sample}]\}$.

Immunofluorescence microscopy

Paraffin embedded tissues were sectioned (10 μ m section thickness) and mounted on superfrost slides. After deparaffinization and antigen retrieval in citrate buffer pH 6.0, immunofluorescence staining on sections was performed using rabbit polyclonal GFP antibody (#2555, 1:1000 dilution; Cell Signalling Technologies) with Alexa Fluor 488 conjugated goat anti-rabbit secondary antibody (#A-11034, 1:200 dilution; Thermo

Fisher), to unambiguously detect eGFP transgene expression and differentiate from tissue background fluorescence.^{8,14} The slides were mounted using a mounting medium containing 4',6-diamidino-2-phenylindole (DAPI) nuclear stain (Fluoro-Gel II, #17985; Electron Microscopy Sciences), and the slides were dried and sealed. Image acquisition was performed using a Zeiss fluorescence microscope under identical conditions (20 \times objective; laser intensity 30%; DAPI exposure time, 50 ms; GFP exposure time, 300 ms). Lumbar spinal cord sections were additionally co-stained for neuronal nuclei protein NeuN using mouse monoclonal NeuN antibody (#MAB377, 1:1000 dilution; Millipore) with Alexa Fluor 568-conjugated goat anti-mouse secondary antibody (#A-11031, 1:200 dilution; Thermo Fisher). The slides were then scanned using NanoZoomer S60 digital slide scanner (Hamamatsu).

Statistics

Quantitative PCR data were analysed in GraphPad Prism software and graph plots were prepared in Microsoft Excel. Data are expressed as arithmetic mean \pm standard error of mean (s.e.m.). Statistical differences in multiple group comparisons were assessed by one-way analysis of variance (ANOVA) *post hoc* Bonferroni test. Pair-wise comparisons were further assessed by Mann-Whitney test, as indicated in figure legends. The alpha level of statistical significance was set at $P = .05$.

Results

rAAV genome was largely detected in the injected muscle and ipsilateral sciatic nerve post injection in hindlimb biceps femoris muscle

To compare the uptake of rAAV serotypes 2/6, 2/8, and 2/9 at the local nerve endings in the muscle and subsequent spreading into the connected nervous structures (as has been proposed for these rAAV serotypes^{13,15,21}), we quantified the rAAV viral genome in different tissues 4 weeks post-i.m. injection (unilateral right hindlimb biceps femoris muscle) in wild-type (C57BL/6J) mice. The rodent sciatic nerve is the largest sensory-motor spinal nerve, and its branches are located deep in the upper hindlimb between the heads of biceps femoris muscle. Accordingly, we investigated the degree of rAAV spreading and transduction efficiency of these select rAAV serotypes into sciatic nerve, L4-L5 DRG (corresponding to the roots of sciatic nerve), lumbar spinal cord, and brain (whole brain homogenate) following i.m. injection. As haematogenous spreading of rAAV6 and rAAV9 has also been reported following i.m. injection in mice,^{14,16} assessment of viral dissemination to liver was also included as a control measurement.

Our results show that the bulk of viral load was detected in the injected biceps femoris muscle, regardless of the rAAV serotype or promoter (ie, CMV or hSyn; Figure 1A). Nevertheless, compared to the un-injected side, significant viral genome could

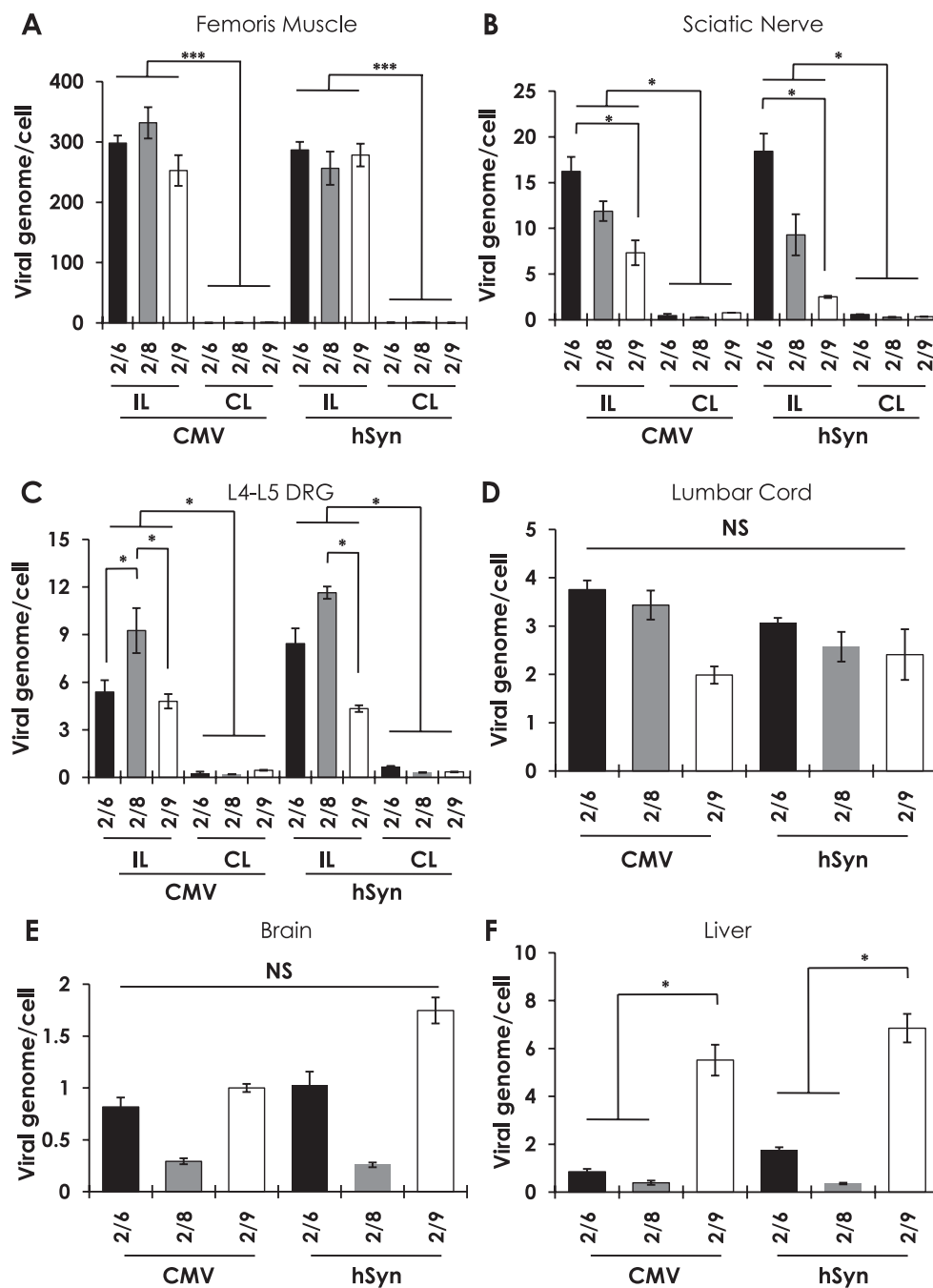


Figure 1. Determination of vector genome copy numbers 4 weeks after a single right hindlimb intramuscular injection of rAAV particles in the injected (biceps femoris) muscle and other tissues. (A) Hindlimb biceps femoris muscle, (B) sciatic nerve, (C) L4-L5 dorsal root ganglia, and lumbar segment of (D) spinal cord, (E) brain, and (F) liver. (2/6, 2/8, and 2/9 indicate respective rAAV serotypes; $n=3$ /group, samples were run in duplicates; multiple group comparisons were assessed by one-way ANOVA post hoc Bonferroni test; pair-wise comparisons were further assessed by Mann-Whitney test; $*P \leq .05$, $***P \leq .005$, only significant differences are highlighted in (A), (B), (C), and (F); NS in (D) and (E), not significant; error bars indicate mean \pm s.e.m.). ANOVA indicates analysis of variance; CL, contralateral – uninjected side; CMV, cytomegalovirus promoter; hSyn, human synapsin promoter; IL, ipsilateral – injected side; rAAV, recombinant adeno-associated virus; s.e.m., standard error of mean.

also be detected in sciatic nerve (Figure 1B) and L4-L5 DRG (Figure 1C) with all the rAAV serotypes tested and was particularly pronounced with rAAV serotypes 2/6 and 2/8. Minimal rAAV viral genome was detected in the lumbar segment of spinal cord or brain in all groups (Figure 1D and E), suggesting limited rAAV spreading. Of the select serotypes, only rAAV2/9 exhibited significant presence of viral genome in the liver

(Figure 1F), and this is not surprising as muscle is a highly vascularised tissue and haematogenous spreading of rAAV9 is well known.^{8,22} These data (Figure 1, also see Table 1) show that although the rAAV genome was predominantly detected in the injected biceps femoris muscle, the select rAAV serotypes exhibited noticeable degree of spreading into the local nervous tissues, particularly into the sciatic nerve and DRG.

Table 1. Viral genome/cell in indicated tissues.

TISSUE	RAAV SEROTYPE, PROMOTER	MEAN VG/ CELL \pm S.E.M.
Femoris muscle (injected side)	2/6, CMV	298.0 \pm 12.5
	2/8, CMV	331.5 \pm 25.9
	2/9, CMV	252.5 \pm 25.4
	2/6, hSyn	286.8 \pm 13.2
	2/8, hSyn	256.3 \pm 27.5
	2/9, hSyn	278.1 \pm 18.8
Sciatic nerve (injected side)	2/6, CMV	16.2 \pm 1.6
	2/8, CMV	11.9 \pm 1.1
	2/9, CMV	7.3 \pm 1.3
	2/6, hSyn	18.4 \pm 1.9
	2/8, hSyn	9.3 \pm 2.2
	2/9, hSyn	2.5 \pm 0.1
L4-L5 DRG (injected side)	2/6, CMV	5.3 \pm 0.7
	2/8, CMV	9.2 \pm 1.4
	2/9, CMV	4.8 \pm 0.4
	2/6, hSyn	8.3 \pm 0.9
	2/8, hSyn	11.6 \pm 0.4
	2/9, hSyn	4.3 \pm 0.2
Lumbar cord	2/6, CMV	3.8 \pm 0.2
	2/8, CMV	3.4 \pm 0.3
	2/9, CMV	2.0 \pm 0.2
	2/6, hSyn	3.1 \pm 0.1
	2/8, hSyn	2.6 \pm 0.3
	2/9, hSyn	2.4 \pm 0.5
Brain	2/6, CMV	0.8 \pm 0.1
	2/8, CMV	0.3 \pm 0.02
	2/9, CMV	1.0 \pm 0.03
	2/6, hSyn	1.0 \pm 0.1
	2/8, hSyn	0.3 \pm 0.02
	2/9, hSyn	1.7 \pm 0.1
Liver	2/6, CMV	0.8 \pm 0.1
	2/8, CMV	0.4 \pm 0.1
	2/9, CMV	5.5 \pm 0.6
	2/6, hSyn	1.7 \pm 0.1
	2/8, hSyn	0.4 \pm 0.03
	2/9, hSyn	6.9 \pm 0.6

Abbreviations: CMV, cytomegalovirus promoter; DRG, dorsal root ganglia; hSyn, human synapsin promoter; rAAV, recombinant adeno-associated virus; s.e.m., standard error of mean; VG, viral genome/cell.

Intramuscular injection of rAAV2/6, 2/8, or 2/9 expressing eGFP under CMV promoter (CMV:eGFP) efficiently transduces biceps femoris muscle and local nervous structures

Then, we wanted to evaluate transduction efficiency, as well whether transgene (ie, eGFP mRNA) expression is influenced by CMV or hSyn promoter in the tissues. We found that the select rAAV serotypes (CMV:eGFP) i.m. inoculation resulted in robust eGFP transgene expression in the ipsilateral biceps femoris muscle of all animals (Figure 2A). In addition, all the tested serotypes caused enhanced eGFP mRNA expression in the ipsilateral (IL) sciatic nerve and L4-L5 DRG compared to the contralateral (CL) side. Specifically, there was >20-fold increase in eGFP mRNA in the sciatic nerve, which was more pronounced with rAAV2/6 (Figure 2B). In the L4-L5 DRG, there was ~2- to 3-fold increase in eGFP mRNA expression in all samples (Figure 2C). In the spinal cord lumbar segment, minimal eGFP mRNA expression was detected, with only rAAV2/6 leading to noticeable expression (~5- to 6-fold; Figure 2D). In addition, there was no detectable eGFP mRNA in brain or liver (Figure 2D). These data show that eGFP expression was predominantly localized in the biceps femoris muscle and sciatic nerve on the injected side, with comparatively lower expression in ipsilateral DRG (compare Figure 2A and B and C and D).

Next, we examined the eGFP epifluorescence (reflecting protein expression) in these tissues by immunofluorescence microscopy. Supporting the data in Figures 1A and B and 2A and B, clear eGFP epifluorescence was observed in the ipsilateral biceps femoris muscle (Figure 3A; compare CL muscle, Figure S1a) and sciatic nerve (Figure 3B; compare CL nerve, Figure S1b). In ipsilateral L4 DRG, large neuronal bodies were seen to be eGFP positive, particularly in mice inoculated with rAAV2/6 and 2/8 (CMV:eGFP); albeit, many DAPI-labelled cells lacking detectable eGFP epifluorescence were also observed (Figure 3C; compare CL DRG, Figure S1a). Supporting the data on low levels of eGFP expression in lumbar cord (Figure 2D), sparse eGFP epifluorescence was observed bilaterally in ventral horn (VH) and dorsal horn (DH), particularly with rAAV2/6 and rAAV2/9 (Figure 4A and C, respectively), predominantly in a pattern resembling neuronal processes. eGFP fluorescence in rAAV2/8 groups was remarkably absent (Figure 4B). These observations are similar to previous studies showing minimal eGFP expression in CL DRG or spinal cord following i.m. injections with rAAV2/6 and 2/8 in adult rodents^{14,15} or in non-human primates.¹³

Biceps femoris muscle injection of rAAV2/6, 2/8, or 2/9 expressing eGFP under human synapsin promoter (hSyn:eGFP) efficiently transduces local nervous structures

Next, we analysed eGFP mRNA and eGFP epifluorescence in the tissues subsequent to biceps femoris muscle i.m. injection with the select rAAV serotypes expressing eGFP under

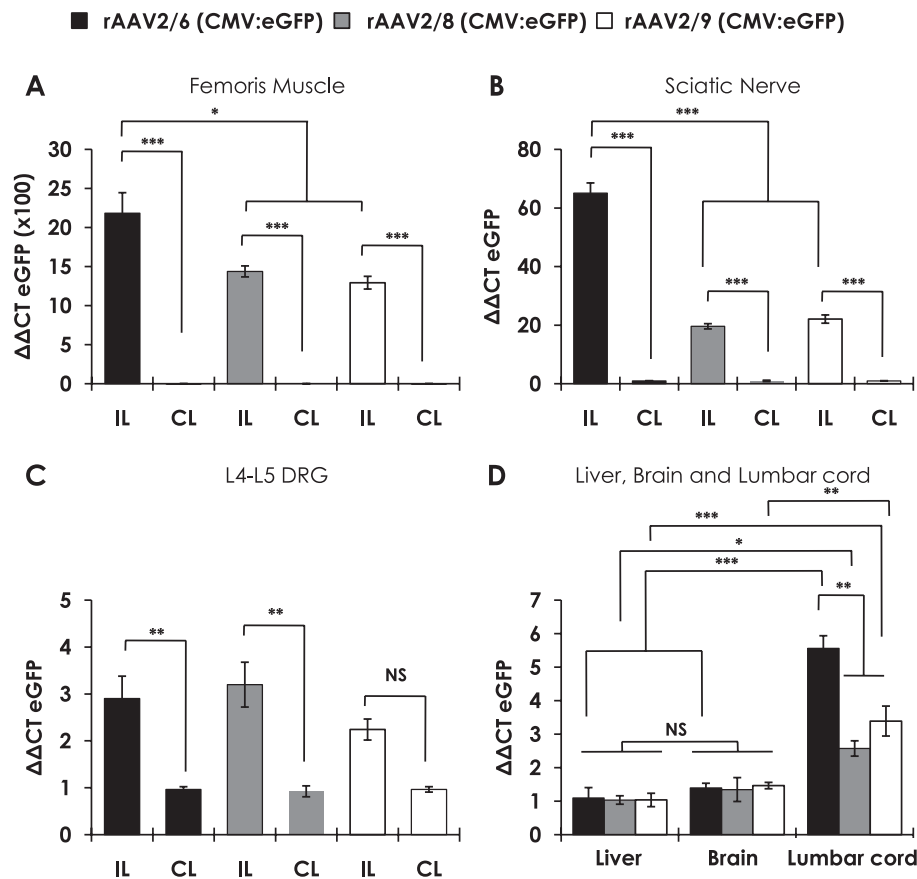


Figure 2. RT-PCR to determine enhanced green fluorescent protein (eGFP) mRNA expression in the injected (biceps femoris) muscle and other tissues 4 weeks following unilateral hindlimb intramuscular delivery of rAAV2/6, 2/8, or 2/9 (CMV:eGFP). (A) Hindlimb biceps femoris muscle; (B) sciatic nerve; (C) L4-L5 dorsal root ganglia; and (D) liver, brain, and lumbar spinal cord segment. (eGFP mRNA relative $\Delta\Delta\text{CT}$ quantification was performed using mouse *gapdh* as the reference gene; data for rAAV2/6 are shown as black bars, data for rAAV2/8 are shown as grey bars, and data for rAAV2/9 are shown as white bars; $n=3/\text{group}$, samples were run in duplicates; qPCR data in (D) were normalized to liver; multiple group comparisons were assessed by one-way ANOVA post hoc Bonferroni test; pair-wise comparisons were further assessed by Mann-Whitney test; $*P \leq .05$, $**P \leq .01$, and $***P \leq .005$, only significant differences are highlighted in (A) to (C); NS in (D), not significant; error bars indicate mean \pm s.e.m.). CL indicates contralateral – uninjected side; CMV, cytomegalovirus promoter; eGFP, enhanced green fluorescent protein; IL, ipsilateral – injected side; qPCR, quantitative PCR; rAAV, recombinant adeno-associated virus.

the control of hSyn promoter (hSyn:eGFP). We found significantly increased eGFP mRNA in the injected muscle (5- to 25-fold, Figure 4A), although not as pronounced as seen with rAAV expressing eGFP under CMV promoter (1300- to 2100-fold; compare Figures 2A and 5A). Furthermore, there was a significantly larger increase in the eGFP mRNA in the ipsilateral sciatic nerve, particularly with rAAV2/6 (~1900-fold) and rAAV2/8 (~140-fold) in hSyn:eGFP groups compared to CMV:eGFP groups (compare Figures 2B and 5B). We also observed 2- to 3-fold increased eGFP mRNA expression in ipsilateral DRG, particularly with rAAV2.6 and 2/8 (Figure 5C). In the lumbar spinal cord, rAAV2/6 led to a robust (~15-fold) increase in eGFP mRNA expression, followed by rAAV2/9 (~5-fold; Figure 5D). In addition, eGFP mRNA was not detectable in brain or liver tissue (Figure 4D). Subsequent eGFP immunofluorescence analyses showed that in the ipsilateral muscle tissue, muscle cell cytoplasm exhibited minimal eGFP epifluorescence, and the pattern of intense eGFP signal on/around the surface of

muscle fibres was reminiscent of nerve terminals in the muscle (Figure 6A; compare CL muscle, Figure S1a). There was visibly pronounced eGFP signal in the ipsilateral sciatic nerve, especially with rAAV2/6 (Figure 6B; compare CL nerve, Figure S1b). As seen with rAAV-CMV:eGFP (Figure 3C), eGFP-positive large neuronal cell bodies in the ipsilateral L4 DRG could be distinguished (Figure 6C; compare CL DRG, Figure S1c). The lumbar spinal cord showed less pronounced eGFP fluorescence, which was scattered bilaterally in both VH and DH, and highlighted neuronal processes (rAAV2/6 and rAAV2/9; Figure 7A and C, respectively). Lumbar cord section from rAAV2/8 mice was largely devoid of any detectable eGFP fluorescence (Figure 7B). Overall, these data suggest limited rAAV transport from i.m. site into lumbar spinal cord regardless of the serotypes used in this study or promoter, with the exception of rAAV2/6 which led to 5- to 15-fold increase in eGFP mRNA expression (Figures 2D and 5D) and appreciable eGFP fluorescence (Figures 4A and 7A).

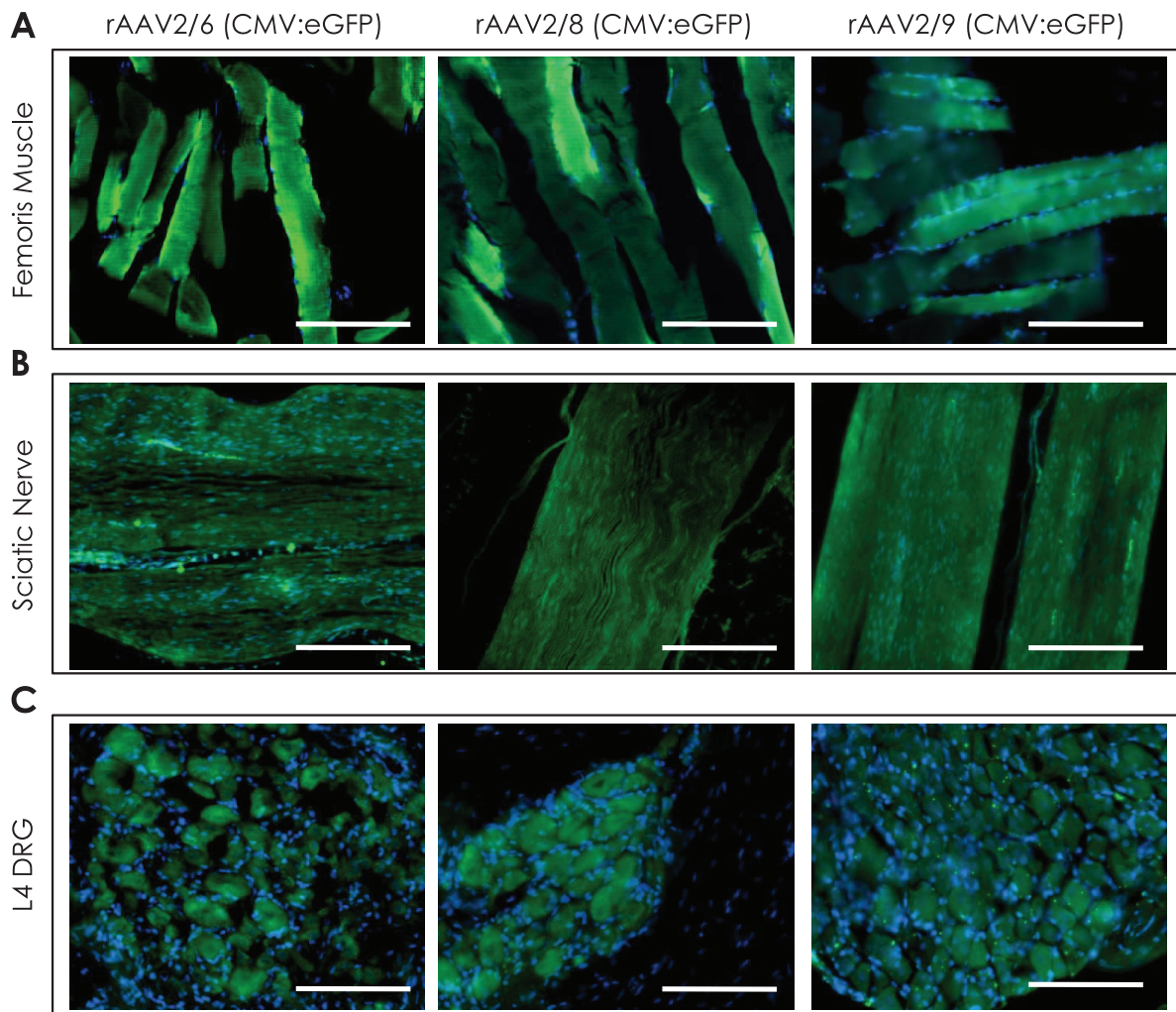


Figure 3. eGFP immunofluorescence in the injected (biceps femoris) muscle and other tissues on ipsilateral side 4 weeks following unilateral hindlimb intramuscular delivery of rAAV2/6, 2/8, or 2/9 (CMV:eGFP). Representative images showing eGFP immunofluorescence (green) in the (A) right hindlimb biceps femoris muscle, (B) right sciatic nerve, and (C) right L4 dorsal root ganglia (DRG) of mice injected with indicated rAAV serotypes. DAPI (blue) was used as a nuclear stain (20 \times magnified view; scale bar=100 μ m). Also see Figure S1 containing data for contralateral side (rAAV2/6-CMV:eGFP). CMV indicates cytomegalovirus promoter; DRG, dorsal root ganglia; eGFP, enhanced green fluorescent protein; rAAV, recombinant adeno-associated virus.

Discussion

Harnessing the capability of some rAAV serotypes for retrograde transduction,^{13,15} whereby the rAAV particles are taken up at the nerve endings and spread in connected neuroanatomical tracts, and evolving the rAAV design to improve such capability (as exemplified recently with rAAV-retro),²³ present promising means of targeted gene transfer in peripheral and central nervous system. Our data show that subsequent to a single i.m. injection in hindlimb biceps femoris muscle of adult mice with 3 select neurotrophic rAAV serotypes (ie, rAAV2/6, 2/8 and 2/9), viral genome and transgene expression (ie, eGFP) was predominantly detected in the injected muscle and ipsilateral sciatic nerve (Figures 1, 2, and 5). Compared to these tissues, substantially less viral load and low expression of eGFP mRNA were detected in the ipsilateral spinal L4-L5 DRG and lumbar spinal cord. Fluorescence microscopy analyses revealed that the eGFP immunofluorescence was predominantly localized in large neuronal cell bodies in ipsilateral DRG (Figures 3

and 6). In the lumbar spinal cord, scant but discernible eGFP signal could be observed bilaterally, particularly with rAAV2/6 and rAAV2/9 (Figures 4 and 7).

Our data suggest that rAAV spreading following i.m. delivery, and transgene (eGFP) expression in injected muscle and nervous tissue, occurred in a manner that reflects nervous supply (motor and sensory) to the biceps femoris muscle. Furthermore, the tissue in immediate vicinity (sciatic nerve) showed higher viral load and eGFP expression than relatively distant locations (DRG, spinal cord, and brain), hence indicating rAAV spreading in connected local neuroanatomical tracts and little or no contribution by other routes of spreading (eg, haematogenous spreading – as has been reported for rAAV2/9). It has been suggested that rAAV can retrogradely target DRG through sensory nerve endings in the intrafusal muscle fibres.¹⁴ Furthermore, ~60% of the nerve fibres in muscle are projections from alpha and gamma motor neurons in the VH of spinal cord and that may explain predominant eGFP localization

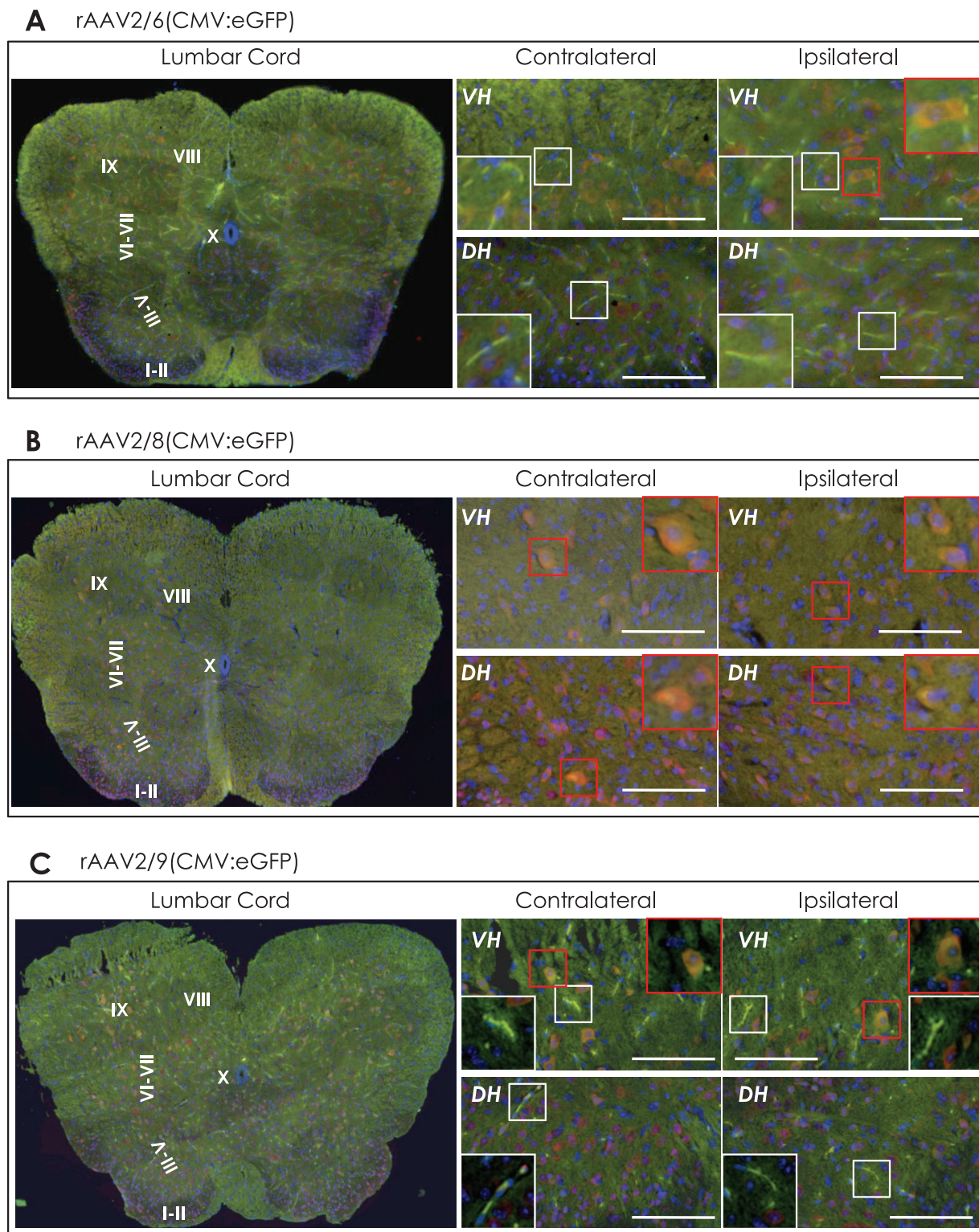


Figure 4. eGFP immunofluorescence in the lumbar spinal cord 4 weeks following unilateral hindlimb intramuscular delivery of rAAV2/6, 2/8, or 2/9 (CMV:eGFP). Representative images showing eGFP immunofluorescence (green) in lumbar spinal cord of mice injected with the rAAV serotypes (A) 2/6, (B) 2/8, or (C) 2/9. The sections were counterstained with NeuN (neuronal nuclei protein, in red) and DAPI nuclear stain (blue). The left panel shows panoramic image (5 \times magnification), and the corresponding high-magnification (20 \times) views in ventral horn lamina IX (VH) and dorsal horn lamina III-V (DH) are presented in the right side panel (scale bar = 100 μ m). The insets show magnified view (80 \times) of neuronal processes (white box) and neuronal cell bodies (red box).

in distinct neuronal populations and neuroanatomical tracts in our study (Figures 3, 4, 6, and 7) and by others.¹³ Our observations are also in line with published reports individually

employing the select rAAV serotypes, delivered in vivo via peripheral routes, for gene transfer in DRG or spinal cord. For instance, i.m. inoculation in adult mice with rAAV2/8

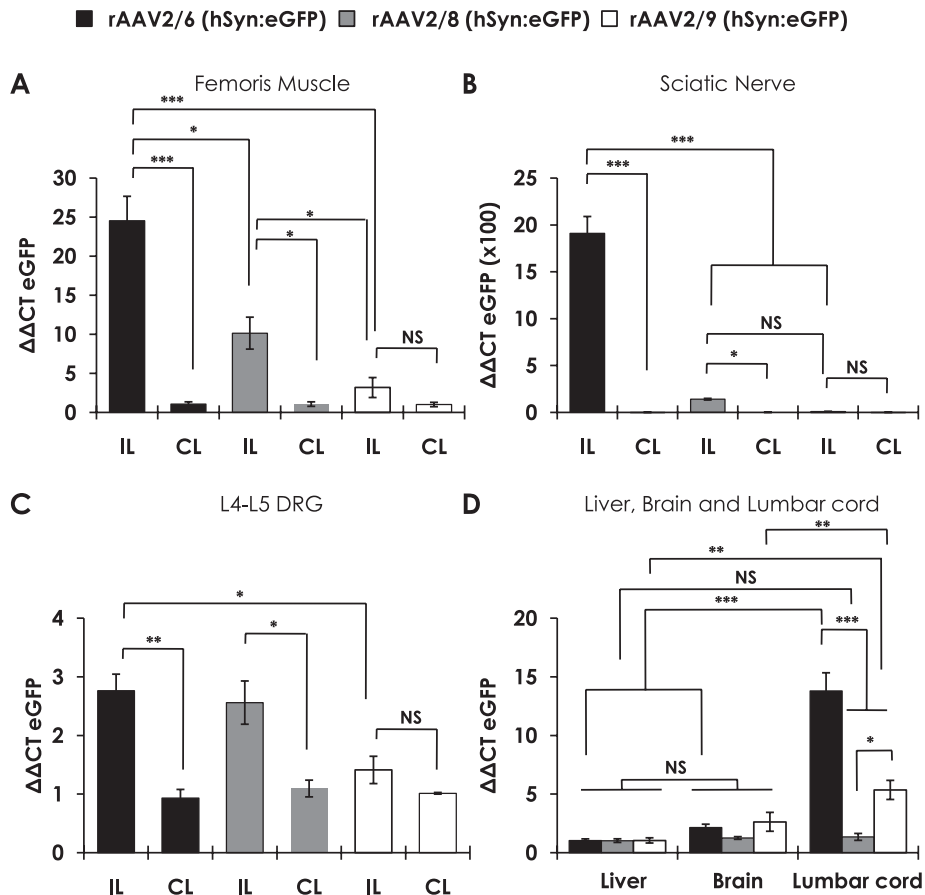


Figure 5. RT-PCR to determine enhanced green fluorescent protein (eGFP) mRNA expression in the injected (biceps femoris) muscle and other tissues 4 weeks following unilateral hindlimb intramuscular delivery of rAAV2/6, 2/8, or 2/9 (hSyn:eGFP). (A) Hindlimb biceps femoris muscle, (B) sciatic nerve, (C) L4-L5 dorsal root ganglia, and (D) liver, brain, and lumbar spinal cord (eGFP mRNA relative $\Delta\Delta\text{CT}$ quantification was performed using mouse *gapdh* as the reference gene; data for rAAV2/6 are shown as black bars, data for rAAV2/8 are shown as grey bars, and data for rAAV2/9 are shown as white bars; $n=3/\text{group}$, samples were run in duplicates; qPCR data in (D) were normalized to liver; multiple group comparisons were assessed by one-way ANOVA post hoc Bonferroni test; pair-wise comparisons were further assessed by Mann-Whitney test; $*P \leq .05$, $**P \leq .01$, and $***P \leq .005$, only significant differences are highlighted; NS in (B) and (D), not significant; error bars indicate mean \pm s.e.m.). CL indicates contralateral uninjected side; eGFP, enhanced green fluorescent protein; hSyn, human synapsin promoter; IL, ipsilateral – injected side; qPCR, quantitative PCR; rAAV, recombinant adeno-associated virus.

encoding eGFP under the control of CMV promoter (CMV:eGFP) has been shown to transduce peripheral nerves in the injected muscle as well as ipsilateral DRG, albeit with limited eGFP expression in spinal cord.¹⁵ Another study compared the rAAV2/6 (CMV:eGFP) viral load and eGFP expression subsequent to s.c. or hindlimb i.m. injection with direct sciatic nerve or intrathecal delivery in spinal cord in adult mice.¹⁴ As expected, the direct modes of delivery resulted in high efficiency, and the authors also found viral delivery in nociceptive neurons in DRG and motor neurons in the lower segments of spinal cord following s.c. or i.m. delivery.¹⁴ In a related study, the same authors also demonstrated robust induction of eGFP expression in motor neurons in the ipsilateral lumbar segments of spinal cord subsequent to a single hindlimb i.m. rAAV2/6 (CMV:eGFP) injection in African green monkeys, somewhat recapitulating the observations in rodents.¹³ A limited number of additional studies have also explored the

transduction of nervous tissues in animal models following peripheral rAAV administration of rAAV1, rAAV2, rAAV9, and self complementary rAAV vectors.²⁴⁻³⁰ These latter studies also showed various degrees of rAAV spreading from the injection site reliant on, ‘hijacking’ the axonal transport machinery, and transduction of neurons in DRG and motor neurons in spinal cord.²⁴⁻²⁷

The lack of widespread dissemination of rAAV following i.m. delivery may be advantageous in studies aimed at targeting local nerve structures, albeit rAAV would have to be delivered bilaterally (for instance, CL nerve or DRG do not show significant viral load or lack of eGFP expression in this study). In addition, our results also show a lack of viral genome or eGFP gene expression in brain, suggesting that the lower limb i.m. delivery route and transport via spinal nerves may not be ideal for that purpose. It would be interesting to determine whether rAAV injections in the territory of a cranial nerve in head and

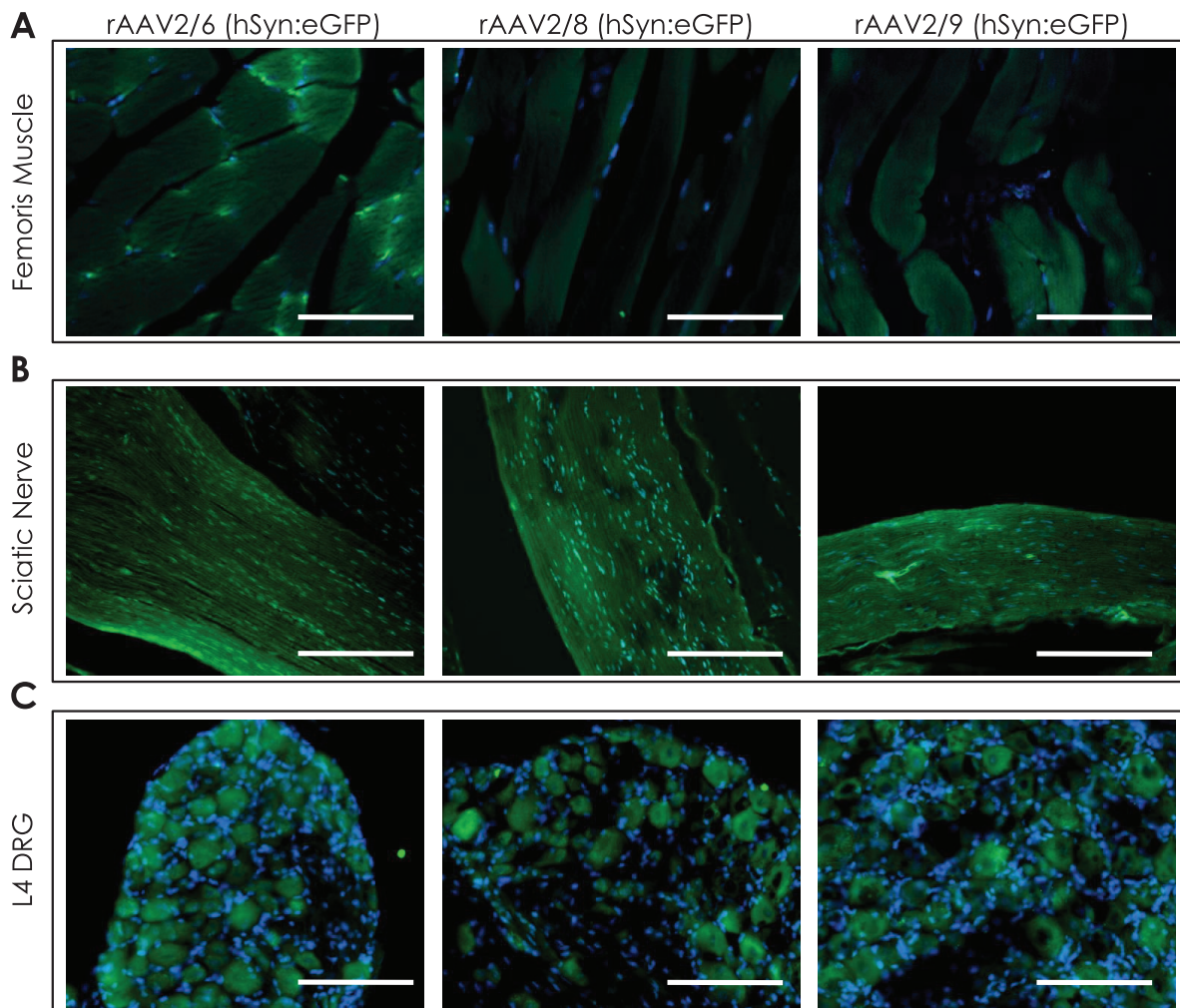


Figure 6. eGFP immunofluorescence in the injected (biceps femoris) muscle and other tissues on ipsilateral side 4 weeks following unilateral hindlimb intramuscular delivery of rAAV2/6, 2/8, or 2/9 (hSyn:eGFP). Representative images showing eGFP immunofluorescence (green) in the (A) right hindlimb biceps femoris muscle, (B) right sciatic nerve, and (C) right L4 dorsal root ganglia (DRG) of mice injected with indicated rAAV serotypes. DAPI (blue) was used as a nuclear stain; 20 \times magnified view; scale bar=100 μ m. Also see Figure S1 containing data for contralateral side (rAAV2/6-hSyn:eGFP). DRG indicates dorsal root ganglia; eGFP, enhanced green fluorescent protein; hSyn, human synapsin promoter; rAAV, recombinant adeno-associated virus.

neck region can lead to rAAV spreading into targeted areas in brain due to proximity (ie, shorter neural tracts). Alternatively, it is also worthwhile to investigate the utility of smooth muscle injections in the territory of large cranial nerve such as vagus in gene transfer into brain, particularly with the refined rAAV pseudotypes, for example, AAV-PHB.eB and AAV-PHP.S¹¹ and rAAV2-retro.²³

Apart from the research utility in basic neuroscience studies, our findings encourage rAAV-mediated disease model development or gene delivery in some models of neurological diseases, for example: (1) rAAV i.m. delivery, particularly with rAAV2/6 and 2/8, can be used for gene transfer in the peripheral nervous system in a targeted manner such that only the local nerves and DRG are transduced.¹⁴ This can be useful in interrogating function of specific genes in models of sensory dysfunction such as neuropathic pain, or for therapeutic gene delivery following nerve injury, and possibly in models of demyelinating diseases, and (2) in models of chronic

neurodegenerative diseases such as Parkinson disease, where misfolded forms of protein aggregates are putatively thought to originate in periphery and spread from peripheral to central nervous system.³¹ In such models, rAAV could be useful in blocking the expression of genes favouring the spreading of misfolded proteins in neuroanatomical tracts affected early in the pathogenesis, as well as for delivering protective genes in peripheral nerves to prevent the toxicity of misfolded protein aggregates originating in periphery.

In conclusion, we compared 3 common rAAV serotypes (rAAV2/6, 2/8, and 2/9 – CMV or hSyn promoter), which have been shown to transduce nerve structures following peripheral routes of delivery, and confirm their utility in achieving gene transfer in local neuroanatomical tracts following hindlimb i.m. inoculation. However, further refinements in rAAV design, combined with alternative strategies in i.m. delivery, maybe required for this route to be satisfactorily useful in targeting selected neuronal populations in spinal cord and brain.

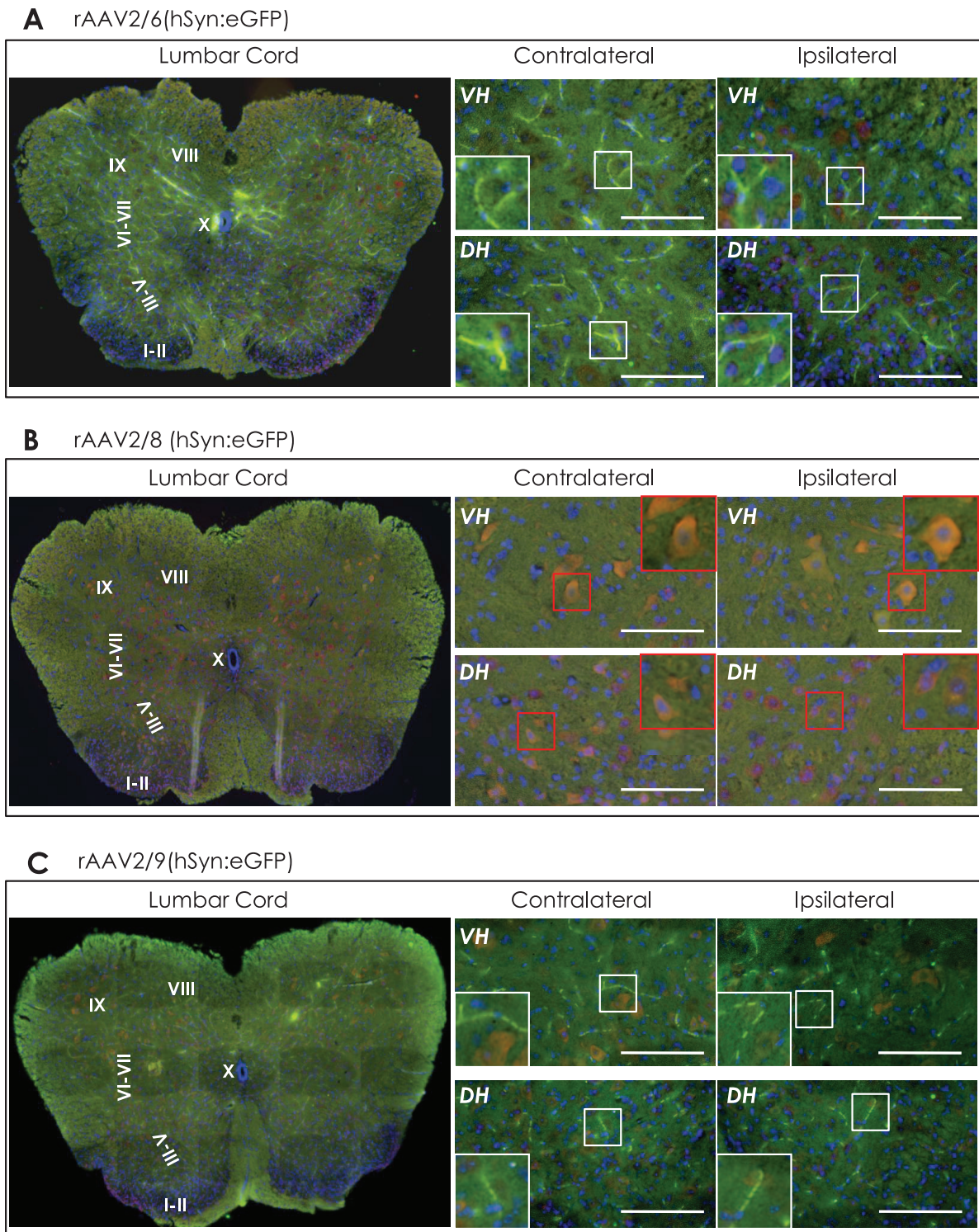


Figure 7. eGFP immunofluorescence in the lumbar spinal cord 4 weeks following unilateral hindlimb intramuscular delivery of rAAV2/6, 2/8, or 2/9 (hSyn:eGFP). Representative images showing eGFP immunofluorescence (green) in lumbar spinal cord of mice injected with the rAAV serotypes 2/6 (A), 2/8 (B), or 2/9 (C). The sections were counterstained with NeuN (neuronal nuclei protein, in red) and DAPI nuclear stain (blue). The left panel shows panoramic image (5 \times magnification), and the corresponding high-magnification (20 \times) views in ventral horn lamina IX (VH) and dorsal horn lamina III-V (DH) are presented in the right side panel (scale bar = 100 μ m). The insets show magnified view (80 \times) of neuronal processes (white box) and neuronal cell bodies (red box). DH indicates dorsal horn; eGFP, enhanced green fluorescent protein; hSyn, human synapsin promoter; rAAV, recombinant adeno-associated virus; VH, ventral horn.

Acknowledgements

The authors would like to thank Helene Andersen (JRN lab) for the help and assistance during the study.

Author Contributions

AJ and PHJ designed the research, AJ and MR performed research, CBV and JRN helped with experimental design and

dataset analysis, and AJ and MR wrote the manuscript. All the authors read and approved the manuscript.

ORCID iD

Asad Jan  <https://orcid.org/0000-0002-3636-0070>

Supplemental material

Supplemental material for this article is available online.

REFERENCES

1. Bedbrook CN, Deverman BE, Gradinaru V. Viral strategies for targeting the central and peripheral nervous systems. *Annu Rev Neurosci.* 2018;41:323-348.
2. Calcedo R, Vandenberghe LH, Gao G, Lin J, Wilson JM. Worldwide epidemiology of neutralizing antibodies to adeno-associated viruses. *J Infect Dis.* 2009;199:381-390.
3. Gao G, Vandenberghe LH, Alvira MR, et al. Clades of adeno-associated viruses are widely disseminated in human tissues. *J Virol.* 2004;78:6381-6388.
4. Hudry E, Vandenberghe LH. Therapeutic AAV gene transfer to the nervous system: a clinical reality. *Neuron.* 2019;101:839-862.
5. Lykken EA, Shyng C, Edwards RJ, Rozenberg A, Gray SJ. Recent progress and considerations for AAV gene therapies targeting the central nervous system. *J Neurodev Disord.* 2018;10:16.
6. Hocquemiller M, Giersch L, Audrain M, Parker S, Cartier N. Adeno-associated virus-based gene therapy for CNS diseases. *Hum Gene Ther.* 2016;27:478-496.
7. Schuster DJ, Dykstra JA, Riedl MS, et al. Biodistribution of adeno-associated virus serotype 9 (AAV9) vector after intrathecal and intravenous delivery in mouse. *Front Neuroanat.* 2014;8:42.
8. Zincarelli C, Soltys S, Rengo G, Rabinowitz JE. Analysis of AAV serotypes 1-9 mediated gene expression and tropism in mice after systemic injection. *Mol Ther.* 2008;16:1073-1080.
9. Lowenstein PR, Mandel RJ, Xiong WD, Kroeger K, Castro MG. Immune responses to adenovirus and adeno-associated vectors used for gene therapy of brain diseases: the role of immunological synapses in understanding the cell biology of neuroimmune interactions. *Curr Gene Ther.* 2007;7:347-360.
10. Foust KD, Nurre E, Montgomery CL, Hernandez A, Chan CM, Kaspar BK. Intravascular AAV9 preferentially targets neonatal neurons and adult astrocytes. *Nat Biotechnol.* 2009;27:59-65.
11. Chan KY, Jang MJ, Yoo BB, et al. Engineered AAVs for efficient noninvasive gene delivery to the central and peripheral nervous systems. *Nat Neurosci.* 2017;20:1172-1179.
12. Shevtsova Z, Malik JM, Michel U, Bahr M, Kugler S. Promoters and serotypes: targeting of adeno-associated virus vectors for gene transfer in the rat central nervous system in vitro and in vivo. *Exp Physiol.* 2005;90:53-59.
13. Towne C, Schneider BL, Kieran D, Redmond DE Jr, Aebischer P. Efficient transduction of non-human primate motor neurons after intramuscular delivery of recombinant AAV serotype 6. *Gene Ther.* 2010;17:141-146.
14. Towne C, Pertin M, Beggah AT, Aebischer P, Decosterd I. Recombinant adeno-associated virus serotype 6 (rAAV2/6)-mediated gene transfer to nociceptive neurons through different routes of delivery. *Mol Pain.* 2009;5:52.
15. Zheng H, Qiao C, Wang CH, et al. Efficient retrograde transport of adeno-associated virus type 8 to spinal cord and dorsal root ganglion after vector delivery in muscle. *Hum Gene Ther.* 2010;21:87-97.
16. Benkhalifa-Ziyyat S, Besse A, Roda M, et al. Intramuscular scAAV9-SMN injection mediates widespread gene delivery to the spinal cord and decreases disease severity in SMA mice. *Mol Ther.* 2013;21:282-290.
17. Morton DB, Jennings M, Buckwell A, et al; and Joint Working Group on Refinement. Refining procedures for the administration of substances. Report of the BVAAWF/FRAME/RSPCA/UFAW Joint Working Group on Refinement. British Veterinary Association Animal Welfare Foundation/Fund for the Replacement of Animals in Medical Experiments/Royal Society for the Prevention of Cruelty to Animals/Universities Federation for Animal Welfare. *Lab Anim.* 2001;35:1-41.
18. Richner M, Jager SB, Siupka P, Vaegter CB. Hydraulic extrusion of the spinal cord and isolation of dorsal root ganglia in rodents. *J Vis Exp.* 2017;119:e55226.
19. Dirren E, Towne CL, Setola V, Redmond DE Jr, Schneider BL, Aebischer P. Intracerebroventricular injection of adeno-associated virus 6 and 9 vectors for cell type-specific transgene expression in the spinal cord. *Hum Gene Ther.* 2014;25:109-120.
20. Livak KJ, Schmittgen TD. Analysis of relative gene expression data using real-time quantitative PCR and the 2(-Delta Delta C(T)) method. *Methods.* 2001;25:402-408.
21. Low K, Aebischer P, Schneider BL. Direct and retrograde transduction of nigral neurons with AAV6, 8, and 9 and intraneuronal persistence of viral particles. *Hum Gene Ther.* 2013;24:613-629.
22. Gray SJ, Matagne V, Bachaboina L, Yadav S, Ojeda SR, Samulski RJ. Preclinical differences of intravascular AAV9 delivery to neurons and glia: a comparative study of adult mice and nonhuman primates. *Mol Ther.* 2011;19:1058-1069.
23. Tervo DG, Hwang BY, Viswanathan S, et al. A designer AAV variant permits efficient retrograde access to projection neurons. *Neuron.* 2016;92:372-382.
24. Wang LJ, Lu YY, Muramatsu S, et al. Neuroprotective effects of glial cell line-derived neurotrophic factor mediated by an adeno-associated virus vector in a transgenic animal model of amyotrophic lateral sclerosis. *J Neurosci.* 2002;22:6920-6928.
25. Boulis NM, Noordmans AJ, Song DK, et al. Adeno-associated viral vector gene expression in the adult rat spinal cord following remote vector delivery. *Neurobiol Dis.* 2003;14:535-541.
26. Hollis Ii ER, Kadoya K, Hirsch M, Samulski RJ, Tuszynski MH. Efficient retrograde neuronal transduction utilizing self-complementary AAV1. *Mol Ther.* 2008;16:296-301.
27. Cearley CN, Wolfe JH. Transduction characteristics of adeno-associated virus vectors expressing cap serotypes 7, 8, 9, and Rh10 in the mouse brain. *Mol Ther.* 2006;13:528-537.
28. Williams J, Vazquez A, Schwartz A. Prolonged functional optical sensitivity in non-human primate motor nerves following cyclosporine-based immunosuppression and rAAV2-retro mediated expression of ChR2. Paper presented at: 9th International IEEE/EMBS Conference on Neural Engineering (NER); March 20-23, 2019; San Francisco, CA.
29. Williams JJ, Watson AM, Vazquez AL, Schwartz AB. Viral-mediated optogenetic stimulation of peripheral motor nerves in non-human primates. *Front Neurosci.* 2019;13:759.
30. Maimon BE, Diaz M, Revol ECM, et al. Optogenetic peripheral nerve immunogenicity. *Sci Rep.* 2018;8:14076.
31. Uchihara T, Giasson BI, Paulus W. Propagation of Abeta, tau and alpha-synuclein pathology between experimental models and human reality: prions, propagons and propaganda. *Acta Neuropathol.* 2016;131:1-3.